

## Guiding 1.5 $\mu\text{m}$ light in photonic crystals based on dielectric rods

Solomon Assefa,<sup>a)</sup> Peter T. Rakich, Peter Bienstman, Steven G. Johnson, Gale S. Petrich, John D. Joannopoulos, Leslie A. Kolodziejski, Erich P. Ippen, and Henry I. Smith

*Research Laboratory of Electronics, Center for Materials Science and Engineering, Massachusetts Institute of Technology, Cambridge, Massachusetts 02139*

(Received 11 May 2004; accepted 25 October 2004)

Photonic-crystal structures consisting of dielectric rods were designed, fabricated, and optically characterized. The combination of the high refractive-index-contrast GaAs/ $\text{Al}_x\text{O}_y$  material system with electron-beam lithography enabled the fabrication of structures suitable for the optical propagation of 1.5  $\mu\text{m}$  light. Experimental transmission spectra were obtained for structures consisting of a two-dimensional array of rods and line-defect waveguides. Optical measurements confirmed the presence of a photonic band gap, as well as band gap guidance in the line-defect waveguide. A two-stage coupling scheme facilitated efficient optical coupling into the line-defect waveguide. © 2004 American Institute of Physics. [DOI: 10.1063/1.1840107]

Photonic crystals are anticipated to have impact on large-scale photonic integrated-circuits by allowing the creation of compact and efficient devices such as waveguides, splitters, and filters.<sup>1,2</sup> Photonic crystals are dielectric structures having a periodically-modulated index of refraction.<sup>3,4</sup> A waveguide is created by introducing a line-defect within the photonic crystal. While the surrounding periodic arrangement of dielectric material provides a photonic band gap, the line-defect functions as a waveguide by localizing certain frequencies within the photonic band gap.<sup>5</sup>

Although three-dimensional photonic crystals provide complete control for guiding light, two-dimensional (2D) slab structures are simpler to fabricate using planar processing tools. Slab photonic crystals provide band gap confinement in the plane, and index confinement in the vertical direction.<sup>6,7</sup> Previous efforts have almost exclusively focused on photonic crystals consisting of a triangular lattice of holes in dielectric slabs, which have a band gap for TE-like modes.<sup>8–10</sup> This paper reports the design, fabrication, and characterization of the “inverse” structure, a square lattice of dielectric-rods in air. The structure has the unique feature of being a disconnected topology that guides light. Also, the dielectric rod structure is fundamentally different, compared to the hole-based structures, due to the high aspect-ratio and the band gap for TM-like polarization.

In the present work, the photonic crystals are composed of a 2D array of high-index dielectric rods that reside on a low-index layer, as shown schematically in Fig. 1(a). Each dielectric rod consists of a 500 nm thick layer of high-index GaAs, epitaxially bonded to an 800 nm thick layer of low-index  $\text{Al}_x\text{O}_y$ . An additional 700-nm-thick  $\text{Al}_x\text{O}_y$  spacer layer separates the dielectric-rod array from the underlying GaAs substrate. For the photonic crystal, each rod has a diameter of 285 nm and is placed in a square lattice with a period of 500 nm. A linear waveguide is created by reducing to 235 nm the diameter of a row of rods, forming a line-defect within the photonic crystal, as seen in Fig. 1(a). The surrounding 2D array of larger diameter GaAs rods establishes a 2D photonic band gap (PBG), thereby confining the light within the smaller diameter defect-row waveguide. In the direction nor-

mal to the plane of periodicity, light is index-confined in the defect rods since each GaAs layer is between low-index  $\text{Al}_x\text{O}_y$  and air.

To create the photonic-crystal waveguide devices, a GaAs/ $\text{Al}_{0.9}\text{Ga}_{0.1}\text{As}$  heterostructure was grown by gas-source molecular-beam epitaxy on a GaAs substrate. Then, 300 nm of  $\text{SiO}_2$  was sputter-deposited onto the III–V substrate. The photonic crystals were defined with scanning-electron-beam lithography using polymethylmethacrylate (PMMA) resist. The PMMA was developed in a 1:2 solution of methyl-isobutyl-ketone (MIBK) and isopropanol (IPA). Next, a 35 nm thick nickel film was evaporated onto the samples and a liftoff process was performed using a heated bath of 1-methyl-2-pyrrolidone (NMP). The nickel was used as a hard mask to transfer the pattern into the  $\text{SiO}_2$  by reactive-ion etching (RIE) in a  $\text{CHF}_3$  plasma. The nickel mask was removed in a wet nickel etchant.

Using the  $\text{SiO}_2$  mask, the dielectric rods were created by etching the GaAs and the underlying  $\text{Al}_{0.9}\text{Ga}_{0.1}\text{As}$  to a total depth of 1.5  $\mu\text{m}$  in a  $\text{BCl}_3$  plasma. The III–V etching step was difficult due to the small feature size, the greater than 5:1 aspect ratio, and the desire to achieve a straight sidewall profile with low sidewall roughness. Using a low dc bias and low pressure during the RIE process, an etch rate of 70 nm/min and 55 nm/min was obtained for the GaAs and  $\text{Al}_{0.9}\text{Ga}_{0.1}\text{As}$  layers, respectively.

Upon completion of the etching, each sample was cleaved to create smooth input and output facets for optical testing. The  $\text{Al}_{0.9}\text{Ga}_{0.1}\text{As}$  was transformed into the low-index  $\text{Al}_x\text{O}_y$  layer using a wet thermal oxidation process. Steam

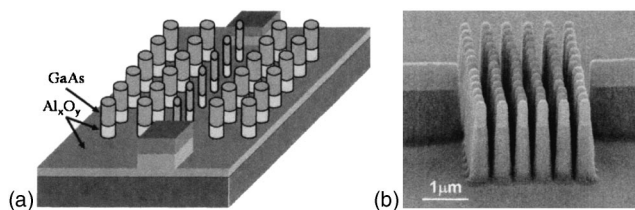


FIG. 1. (a) Schematic illustrating a 2D array of dielectric rods, conventional dielectric input/output waveguides, and a line-defect waveguide. (b) Side-view scanning-electron microscope (SEM) image of a photonic crystal after the final RIE and oxidation steps.

<sup>a)</sup>Electronic mail: Solomona@mit.edu

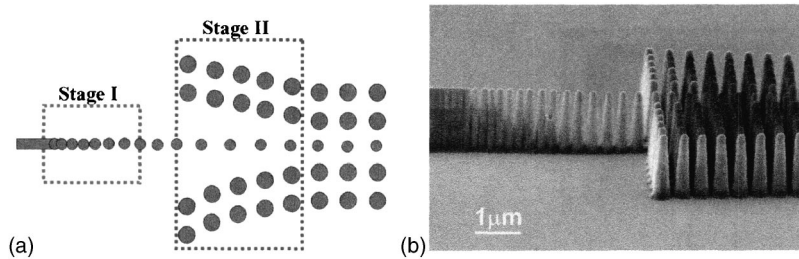


FIG. 2. (a) Top-view schematic of a two-stage coupling structure. (b) Side-view SEM image of the structure after the final RIE and oxidation steps.

from a H<sub>2</sub>O bath, heated to 90 °C, was introduced into the oxidation furnace using N<sub>2</sub> as a carrier gas. An oxidation temperature of 435 °C resulted in an oxidation rate of ~40 nm/min. As the oxidation time required for the aforementioned structures is short, the oxidation process is reaction-rate-limited (linear regime). Figure 1(b) shows a scanning-electron microscope (SEM) image of a bulk photonic-crystal device after fabrication.

Light can be coupled directly from a fiber to a rod-based photonic-crystal waveguide by encapsulating the structure with a low index polymer.<sup>11</sup> However, a carefully designed modal transformation is required to achieve efficient coupling from a conventional high-index-contrast input waveguide to a photonic-crystal defect-row waveguide.<sup>12,13</sup> As reported in the literature, a gradual taper transition may offer a potential mechanism to couple light from conventional waveguides into photonic crystal waveguides.<sup>14,15</sup> Without a proper coupling design, the transition to the defect-row waveguide was found to suffer from Fabry–Perot reflections, resulting in transmission that is dependent on frequency and the length of the photonic-crystal waveguide.

To facilitate coupling from a conventional high-index-contrast waveguide into the photonic-crystal line-defect waveguide, a two-stage coupling scheme was employed, as shown schematically in Fig. 2(a). The forward propagating optical mode in the conventional dielectric waveguide was adiabatically transformed into a combination of forward and backward propagating field components prior to coupling into the photonic-crystal defect-row waveguide.<sup>16,17</sup> The transformation is accomplished by transitioning from a single-mode strip waveguide into a waveguide consisting of a one-dimensional (1D)-periodic sequence of rods (index-guided both in-plane and vertically) with a fixed period and having the same radius as the final line-defect of rods (Stage I). This 1D-rod waveguide is transformed into a 2D photonic-crystal line-defect waveguide by the inclusion of the surrounding 2D photonic crystal (Stage II). Elimination of an abrupt photonic crystal interface avoids reflection; hence, the transition from the 1D-rods to the line-defect waveguide is accomplished by gradually reducing the distance between the cladding photonic crystal and the 1D-rod waveguide [Fig. 2(a)]. The input portion of a complete device, ready for optical testing, is shown in Fig. 2(b); the SEM image shows the input waveguide, the two-stage coupling scheme, and the photonic crystal defect-row waveguide. The output side of the device is the mirror of the input portion of the device that is seen in Fig. 2(b).

Optical characterization of the devices was accomplished using a computer-controlled laser, tunable from 1430 to 1610 nm. The sample was mounted on a translation stage capable of 10 nm resolution, and TM-polarized light was coupled into the waveguide with a high-numerical-aperture fiber-lens assembly. The waveguide output was first spatially

filtered, and then analyzed with a polarizing beamsplitter. Transmission spectra were obtained by measuring the output signal with photodetectors while tuning the wavelength of the laser. Also, the waveguides were imaged from the top to observe any reflection at the photonic-crystal interface and radiation loss due to waveguide damage.

Figure 3(a) shows the transmission as a function of wavelength measured across a 2D photonic-crystal device having two and four rows of rods. The creation of a photonic band gap, from 1448 to 1482 nm, is observed in the case of four rows of rods. Time-domain simulation of the device showed a band gap with a similar bandwidth but with a 3% shift in wavelength. Figure 3(b) shows the measured transmission spectrum for a photonic-crystal line-defect waveguide that utilizes the aforementioned two-stage coupling scheme on both the input and the output. For two represen-

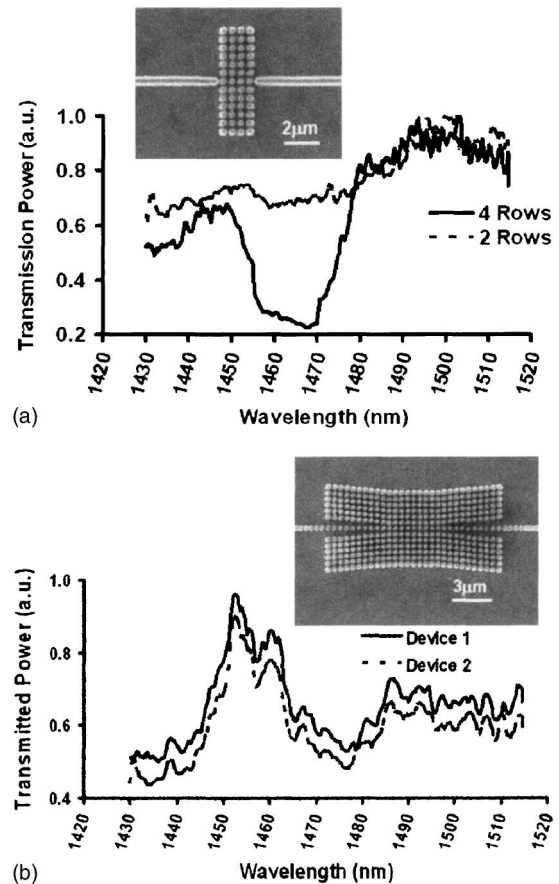


FIG. 3. (a) Measured transmission spectra as a function of wavelength for photonic-crystal structures with two and four rows of rods. The structure with four rows exhibits a band gap for the wavelength range of 1448–1482 nm. (b) Measured transmission spectra for line-defect waveguides with the two-stage coupling scheme demonstrate guiding inside the band gap. The measurement was reproducible for two similar devices on the same chip. The measured structures are illustrated by the inset SEM images.

tative devices, an increase in transmission is observed within the measured band gap, demonstrating lateral guiding of light due to the photonic band gap rather than total internal reflection. The spectral features obtained from the bulk photonic crystal devices and the two-stage taper devices were very reproducible for many similar devices on the same chip.

In summary, GaAs-based dielectric rod arrays were utilized to fabricate photonic-crystal devices that allow the propagation of 1.5  $\mu\text{m}$  light. Optical transmission measurements confirmed the presence of a photonic band gap for a photonic crystal consisting of only four rows of rods. Furthermore, a two-stage coupling scheme was employed to couple light from a conventional waveguide to a photonic-crystal defect-row waveguide. Optical measurements demonstrated light was coupled into the line-defect waveguide and confined laterally by the band gap.

This work was supported primarily by the MRSEC Program of the National Science Foundation under Award No. DMR 02-13282. The authors gratefully acknowledge the contributions from M. Mondol regarding electron beam lithography.

<sup>1</sup>Attila Mekis, J. C. Chen, I. Kurkland, Shanhui Fan, Pierre R. Villeneuve, and J. D. Joannopoulos, *Phys. Rev. Lett.* **77**, 3787 (1996).

<sup>2</sup>S. Y. Lin, E. Chow, J. Bur, S. G. Johnson, and J. D. Joannopoulos, *Opt.*

*Lett.* **27**, 1400 (2002).

<sup>3</sup>E. Yablonovich, *Phys. Rev. Lett.* **58**, 2059 (1987).

<sup>4</sup>S. John, *Phys. Rev. Lett.* **58**, 2486 (1987).

<sup>5</sup>J. Joannopoulos, R. Meade, and J. Winn, *Photonic Crystals: Molding the Flow of Light* (Princeton University Press, Princeton, 1995).

<sup>6</sup>S. G. Johnson, S. Fan, P. R. Villeneuve, J. D. Joannopoulos, and L. A. Kolodziejski, *Phys. Rev. B* **60**, 5751 (1999).

<sup>7</sup>S. G. Johnson and J. D. Joannopoulos, *Appl. Phys. Lett.* **77**, 3490 (2000).

<sup>8</sup>D. Labilloy, H. Benisty, C. Weisbuch, T. F. Krauss, R. M. De La Rue, V. Bardinal, R. Houdre, U. Oesterle, D. Cassagne, and C. Jouanin, *Phys. Rev. Lett.* **79**, 4147 (1997).

<sup>9</sup>C. J. M. Smith, H. Benisty, S. Olivier, M. Rattier, C. Weisbuch, T. F. Krauss, R. M. De La Rue, R. Houdre, and U. Oesterle, *Appl. Phys. Lett.* **77**, 2813 (2000).

<sup>10</sup>S. Y. Lin, E. Chow, S. G. Johnson, and J. D. Joannopoulos, *Opt. Lett.* **25**, 1297 (2000).

<sup>11</sup>M. Tokushima, H. Yamada, and Y. Arakawa, *Appl. Phys. Lett.* **84**, 4298 (2004).

<sup>12</sup>Attila Mekis and J. D. Joannopoulos, *J. Lightwave Technol.* **19**, 861 (2001).

<sup>13</sup>Yong Xu, Reginald K. Lee, and Amnon Yariv, *J. Opt. Soc. Am.* **25**, 755 (2000).

<sup>14</sup>T. D. Happ, M. Kamp, and A. Forchel, *Opt. Lett.* **26**, 1102 (2001).

<sup>15</sup>Philippe Lalanne and A. Talneau, *Opt. Express* **10**, 354 (2002).

<sup>16</sup>Peter Bienstman, Solomon Assefa, S. G. Johnson, J. D. Joannopoulos, G. S. Petrich, and L. A. Kolodziejski, *J. Opt. Soc. Am. B* **20**, 1817 (2003).

<sup>17</sup>S. G. Johnson, Peter Bienstman, M. A. Skorobogatiy, Mihai Ibanescu, Eleftherios Lidorikis, and J. D. Joannopoulos, *Phys. Rev. E* **66**, 066608 (2002).